ELSEVIER

Journal of Photochemistry and Photobiology A: Chemistry 131 (2000) 85–94

Journal of Photochemistry and Photobiology A:Chemistry

www.elsevier.nl/locate/jphotochem

Theoretical studies on mechanism of primary electronic transfer in the photosynthetic reaction center of *Rhodopseuodomonas Virid*

Xiao-dong Zhang, Shu-hua Ma, Yan-ni Wang, Xing-kang Zhang, Qi-yuan Zhang *

State Key Laboratory for Structural Chemistry of Unstable & Stable Species, Institute of Chemistry, Chinese Academy of Sciences, Beijing 100080, China

Received 9 June 1999; received in revised form 27 September 1999; accepted 10 October 1999

Abstract

The electronic structure of the primary electron donor, P960, in photosynthetic reaction center (RC) of *Rhodopseudomonas* (*Rps.*) *Virid* has been studied with the ab initio method at the minimal basis set and the restricted Hartree–Fock (RHF) level by using the Gaussian 98 program. The effect of the surrounding proteins and the histidine residue axial ligands on the electronic structure of super-molecule P960 has also been studied. The results indicated: (1) For super-molecule P960, the LUMOs mainly consist of atomic orbitals (AOs) of atoms in *BChl* b_L, its corresponding HOMOs mainly come from the contributions of AOs of atoms in *BChl* b_M. The surrounding proteins and histidine residue axial ligands do not change the compositions of its HOMO and LUMO significantly. These results are helpful to understand the fact that the primary ET process in RC of *Rps. Virid* only takes place along the L branch; and (2) According to the relative positions of E_{LUMO}s of the primary electron donor P960, P960-h and pigment molecules *ABChl*, *ABChl-h* and *BPheo* located in the L and M subunits in the RC of *Rps. Virid*, respectively, it can also be seen that the primary ET process should take place along the L branch and it should be a one-step process from P960-h to *BPheo* b_L. The coordination of histidine residue axial ligands at P960 and *ABChl b* molecules play a very important role in the primary ET process of the RC of *Rps. Virid*.

Keywords: P960-*Rps. Virid*; Electronic structure; Electron transfer; Ab initio

1. Introduction

Since the X-ray crystal structure (0.23-nm resolution) of photosynthetic reaction center (RC) for *Rhodopseudomonas* (*Rps.*) *Virid* was resolved [1], the studies of the primary electron transfer (ET) process have reached a new level and achieved a great step forward [2–34]. But there still exist some problems about the ET mechanism, which are not understood clearly. Current research focused on the reason why the primary ET process only takes place along the L branch of the pseduo-C_{2v} symmetric bacterial RC, and the role played by the accessory bateriochloropyhll (*ABChl*) in the ET process, etc. In order to investigate the mechanism in detail, many papers [2–26,31–34] have been published from the theoretical point of view. Parson et al. [13] used the molecular mechanics method to calculate the electrostatic interaction between RC and the surrounding proteins and obtained the result that the electrostatic interaction favored the ET along the L branch. Thompson et al. [14–18] calculated the electronic structure and spectra of the pigment molecules in *Rps. Virid* RC by using the ZINDO method and obtained that the charge separation in L branch was favorable in energy. Hasegawa et al. [26] calculated the transfer integral between the primary electron donor P960 and *ABChl* in *Rps. Virid* RC by using the ab initio quantum chemical method SAC-CI, and concluded that the unidirectionality of the ET could be explained by the asymmetry of the transfer integral for ET from P960 to *ABChl* and from *ABChl* to bacteriopheophytin (*BPheo*) between subunits L and M. Many chemists also tried to explore the role played by *ABChl* from the experimental and theoretical point of view, but they obtained different results. The following are a few examples

1. The energy of $ABChlb_L^-$ is about 9 or 15 kcal/mol higher than that of the excited state of P960 and concluded that the *ABChl* is impossible to be an intermediate in the primary ET process [15,18,24,25]. Time-resolved spectrum experiments had been used to detect the reduced *ABChl*, but failed [27,28].
2. The energy of $ABChlb_L^-$ is about 1.0 kcal/mol lower than that of the excited state of P960, so that the

* Corresponding author: Tel.: +86-10-6257-9454; fax: +86-10-62569464.
E-mail address: zhangqy@infoc3.icas.ac.cn (Q.-y. Zhang).

1010-6030/00/$ – see front matter
PII: S1010-6030(99)00216-6

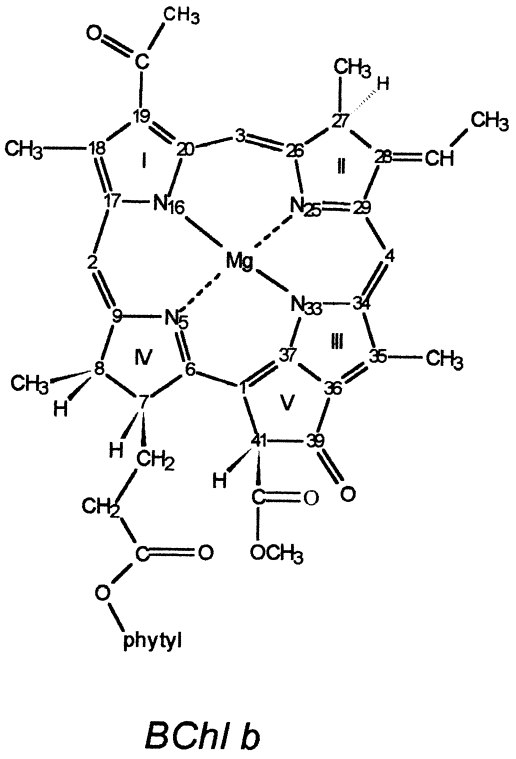

Fig. 1. The topological structural frame of bacteriochlorophyll b (*Bchl b*). The numbers denote these atoms belonging to molecule *BChl* b_L. When they are added to 47, the atoms belong to *BChl* b_M molecule. The Roman numbers denote the ring numbers of pyrrole in *BChl b*.

$ABChlb_L^-$ is really a kinetic intermediate [5–8]. Based on fluorescence experiments [29,30] and dynamics simulations [22,31], the authors thought the primary ET was a two-step ET process.

3. The energy of $ABChlb_L^-$ is similar to that of the excited state of P960 and the electron exchange between them is reversible [7].

When we make a survey of the structure of the RC of *Rps. Virid* in the intermolecular interaction point of view, we can find that it is a super-molecular system of multi-level structure. A pair of bacteriochlorophyll b (*BChl b* shown in Fig. 1) molecules coupled each other to form a super-molecular 'special pair' — the primary electron donor P960. Next to the special pair, there are two *ABChl b* molecules and then two *BPheo b* molecules, and other pigment molecules sequentially, to form subunits A and B, respectively. Furthermore, subunits A and B are connected with the protein scaffolding L and M, respectively, to form a quasi-C_{2v} symmetric super-molecular system. It can be seen that the intermolecular interactions within the special pair P960 are of the primary level one. Interactions between P960 and amino acid molecules, other pigment molecules and the protein surroundings could be of the next levels.

In this paper, firstly we focus our study on the electronic structure of super-molecule P960, *ABChl b* and *BPheo b* molecules in the RC of *Rps. Virid*, and then on the influence of coordinated amino acid molecules and the surrounding proteins on the electron structure of P960 with ab initio quantum chemistry method. Finally, we will search the structural background which causes the fact that the electron transfer only takes place along the L subunit, and to see whether the primary ET is a one- or two-step process.

2. Model and methods of calculations

The crystal structural data of RC of *Rps. Virid*, 1PRC (0.23-nm resolution) [1], were taken from the Brookhaven Protein Databank, organized by the Brookhaven National Laboratory. Two *BChl b* molecules which construct the super-molecule P960, the primary electron donor, (shown in Fig. 2) were denoted by *BChl* b_L and *BChl* b_M, respectively, where subscripts L and M denote molecules connecting with the L and M branches of the surrounding proteins. Molecules *BChl* b_L and *BChl* b_M with histidine residues axially coordinated at their Mg ions were denoted by $BChl\ b_L^h$ and $BChl\ b_M^h$, respectively, and the corresponding super-molecule is denoted by P960-h (shown in Fig. 3). Next to the P960, there are two accessory bacteriochlorophylls b, *ABChl* b_L and *ABChl* b_M, and two bacteriopheophytin b, *BPheo* b_L and *BPheo* b_M, sequentially.

Since hydrogen atoms were not included in the X-ray structure data of *Rps. Virid* RC, they were added by using the program Alchemy III. In the calculation, the amino acid roots (–$CHNH_2COOH$) of coordinated histidines were replaced with hydrogen atoms. The electronic structures of super-molecules mentioned above were calculated with the ab initio method at the minimal basis set and the restricted Hartree–Fock (RHF) level by using the Gaussian 98 program [36]. In the calculations, we found that the influence of phytyl chain on the composition of the frontier molecular orbitals and their energy levels of super-molecule P960 is limited. On the contrary, the composition of the frontier molecular orbitals are changed considerably if any other functional group in super-molecule P960 is replaced with

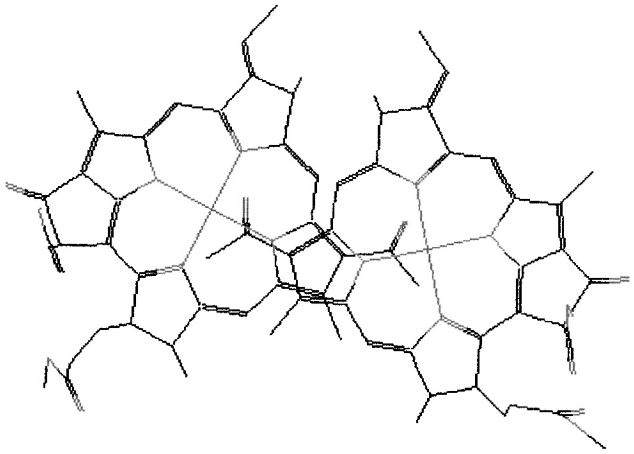

Fig. 2. The structural scheme of super-molecule P960. The purple, red, blue and black represent the Mg, O, N and C atoms, respectively.

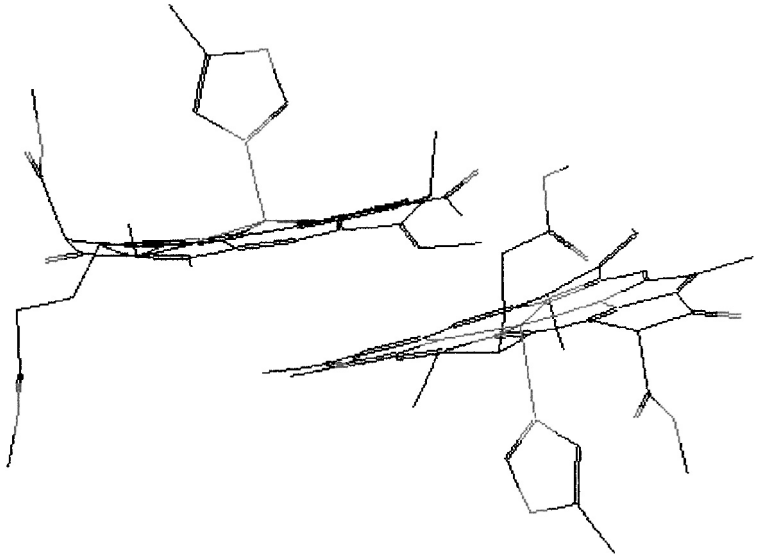

Fig. 3. The structural scheme of super-molecule P960-h. The purple, red, blue and black represent the Mg, O, N and C atoms, respectively.

the H atom. Thus, in our calculation models all functional groups of super-molecules P960, P960-h, *BChl b*, *ABChl b* and *BPheo b* all remain, except for the phytyl ($C_{20}H_{39}$) chain truncated with a methyl.

Since two *BChl* b_L and *BChl* b_M molecules of P960 only partly overlap and the distance between their molecular planes is as large as 0.3 nm, some of their intrinsic characters could be preserved, the electronic structure of each *BChl b* and *BChl* b^h molecule was also calculated. In the calculation of *BChl* b_L (*BChl* b_L^h), the atoms of *BChl* b_M (*BChl* b_M^h) were all isolated from P960 (P960-h) and the others were not changed, and the corresponding isolations were taken in the calculations of *BChl* b_M (*BChl* b_M^h).

The difficulty of quantum chemical treatment for the biological molecular complexes also lies in the simulation of their environment. To approach this problem, the SCRF method [37] were used. According to the SCRF method, spherical cavities with the radii $r = 0.791$ and 0.785 nm were used to surround the super-molecules P960 and P960-h and their composition units, respectively. The surrounding protein was considered as a continuous medium of uniform dielectric constant $\varepsilon = 2.5$ based on the Onsager model. In case of comparison with systems in the DMF solution, $\varepsilon = 36.7$ is also used.

3. Results and discussion

3.1. The energy values and stability

Calculated energy values of the super-molecules (Dimer) P960 and P960-h and their composition units (CUs) in gas and solution phases (by SCRF, $\varepsilon = 2.50$) were listed in Table 1, where subscripts L and M denote the corresponding units connecting with the protein of L and M branches, respectively. *E*u is defined as $Eu = E_L - E_M$, and E_D is the dimerizational energy defined as $E_D = E_L + E_M - E_{Dimer}$.

From Table 1, it follows that for super-molecules P960 and P960-h, the energies of CUs in the L-branch are always lower than those of CUs in the M-branch, respectively, which is in agreement with that in Ref. [3]. The influence of surrounding proteins and histidine residue axial ligands on the values of Eus is limited. The dimerizational energy E_D of P960 is about −0.9 eV, which is also in agreement with that in Ref. [3]. The E_D of P960-h is about −0.7 eV. These results indicate that the two following processes

$$BChlb_L + BChlb_M \rightarrow \text{P960} \quad (1)$$

$$BChlb_L^h + BChlb_M^h \rightarrow \text{P960} - h \quad (2)$$

Table 1
The energy values of primary electron donor (Dimer) and their corresponding units, where subscripts L and M denote the units in the L- and M-branches for P960 and P960-h, respectively. $Eu = E_L - E_M$, and $E_D = E_L + E_M - E_{Dimer}$

		L (a.u.)	M (a.u.)	Eu (eV)	Dimer (a.u.)	E_D (eV)
P960	Gas	−2222.76882	−2222.58666	−4.957	−4445.32427	−0.849
	SCRF ($\varepsilon = 2.50$)	−2222.76923	−2222.58715	−4.955	−4445.32438	−0.871
P960-h	Gas	−2483.38241	−2483.20185	−4.913	−4966.55863	−0.697
	SCRF ($\varepsilon = 2.50$)	−2483.38320	−2483.20291	−4.906	−4966.55870	−0.746

Table 2
The energy levels of the highest occupied molecular orbital (E_{HOMO}) and the lowest unoccupied molecular orbitals (E_{LUMO}) of super-molecules (Dimer) and their composition units, and the corresponding molecular orbital energy gap $\Delta\varepsilon$ ($\Delta\varepsilon = E_{LUMO} - E_{HOMO}$)[a]

			E_{HOMO-1}	E_{HOMO}	E_{LUMO}	E_{LUMO+1}	$\Delta\varepsilon$
P960	Gas	*BChl* b_L	−4.52992	−3.50785	2.23652	5.09401	5.74437
		BChl b_M	−4.77291	−3.53179	2.39544	5.14626	5.92723
		Dimer	−3.66840	−3.55574	1.97774	2.42102	5.53348
	SCRF ($\varepsilon = 2.50$)	*BChl* b_L	−4.52774	−3.51057	2.25611	5.10462	5.76668
		BChl b_M	−4.76856	−3.53724	2.41557	5.15905	5.95281
		Dimer	−3.67520	−3.56526	1.97311	2.41721	5.53838
P960-h	Gas	*BChl* b_L^h	−3.98215	−3.14838	2.61531	5.47307	5.76369
		BChl b_M^h	−4.14650	−3.14267	2.77694	5.53402	5.91961
		Dimer	−3.19655	−3.09586	2.48687	2.93504	5.58273
	SCRF ($\varepsilon = 2.50$)	*BChl* b_L^h	−3.99276	−3.16335	2.63898	5.48287	5.80233
		BChl b_M^h	−4.14569	−3.15410	2.79899	5.54164	5.95308
		Dimer	−3.20308	−3.09750	2.48088	2.93640	5.57838

[a] The subscripts L and M denote the *BChl b* molecules connected with the L and M subunits, respectively. The superscript 'h' represents the histidine residues(units eV).

are endothermic. The influence of surrounding proteins on the values of E_D is not significant.

3.2. Frontier molecular orbital energy levels and energy gaps

Calculated energy levels of the highest occupied molecular orbital (E_{HOMO}) and those of the lowest unoccupied molecular orbital (E_{LUMO}) for super-molecules (Dimer) P960/P960-h and their composition units (CUs) are listed in Table 2. The molecular orbital energy gaps $\Delta\varepsilon$s, defined as $\Delta\varepsilon = E_{LOMO} - E_{HOMO}$, are also shown in Table 2. The values of E_{HOMO}, E_{LUMO} and of *ABChl b* and *BPheo b* are presented in Table 3.

From Tables 2 and 3, it can be seen that:

1. Molecular orbital energy gaps $\Delta\varepsilon$s of super-molecules P960 and P960-h are narrower than those of their CUs, except *BChl* b_L^h in the gas phase. This indicates that super-molecules P960 and P960-h are more photochemically active than their CUs. The influence of the surrounding proteins and the histidine residue axial ligands on these results is not significant.
2. Energy gaps $\Delta\varepsilon$s of the CU Ls of super-molecules P960 and P960-h are narrower than those of their CU Ms, respectively. This indicates that the CU Ls are more photochemically active than those of CU Ms. The influence of the surrounding proteins and the histidine residue axial ligands on $\Delta\varepsilon$s is not significant either.
3. According to the Koopmans theory, we can obtain the electron affinity (EA) from the values of E_{LUMO}s. It can be seen from the results that the EA for *BPheo* b_L and *BPheo* b_M are greater than those of *ABChl* b_L and *ABChl* b_M, respectively. The differences of EAs between *ABChl* b_M and *BPheo* b_M on the one hand, and *ABChl* b_L and *BPheo* b_L, on the other, in the DMF solution ($\varepsilon = 36.7$) are about 2.06 and 2.45 kcal/mol, respectively, which are consistent with those calculated average values of EA for *ABChl b* and *BPheo b* in the L and M branches, namely 2.7 kcal/mol [33] and 2.8 kcal/mol [34]. The differences of EAs between *ABChl* b_M^h and *BPheo* b_M, *ABChl* b_L^h and *BPheo* b_L in DMF solution ($\varepsilon = 36.7$) are about 0.497 and 0.492 eV, respectively, which are also consistent with the calculated average values of EA for *ABChl b* with histidine residue axial ligands and

Table 3
The HOMO and LUMO energy levels of the accessory bacteriochlorophylls b (*ABChl b*) and bacteriopheophytin b (*BPheo b*), and the molecular orbital energy gap $\Delta\varepsilon$, $\Delta\varepsilon = E_{LUMO} - E_{HOMO}$[a]

	Gas			SCRF					
	E_{HOMO}	E_{LUMO}	$\Delta\varepsilon$	E_{HOMO}	E_{LUMO}	$\Delta\varepsilon$	E_{HOMO}	E_{LUMO}	$\Delta\varepsilon$
				$\varepsilon = 2.50$			$\varepsilon = 36.7$		
ABChl b_L	−3.54377	2.40006	5.94383	−3.55030	2.45013	6.00043	−3.56064	2.51109	6.07172
ABChl b_M	−3.42050	2.48061	5.90111	−3.43247	2.54156	5.97403	−3.44172	2.61014	6.05186
ABChl b_L^h	−3.17614	2.83137	6.00750	−3.19437	2.86946	6.06383	−3.21723	2.91899	6.13622
ABChl b_M^h	−3.03056	2.91219	5.94274	−3.05287	2.95273	6.00560	−3.24498	2.99600	6.24098
BPheo b_L	−3.39737	2.37040	5.76777	−3.40825	2.39217	5.80042	−3.42349	2.42183	5.84532
BPheo b_M	−3.23274	2.43544	5.66818	−3.29968	2.46483	5.76451	−3.38104	2.50401	5.88505

[a] The subscripts L and M denote the *BChl b* molecules connected with the L and M subunits, respectively. The superscript 'h' represents the histidine residue axial ligands (units eV).

BPheo b in *L* and *M* branches, 0.38 eV [16–18], and the experimental value, 0.40 eV [35]. *BPheo* b_L molecule is the strongest electron acceptor among these pigments since its EA is the greatest and imply the excited electron from P960/P960-h will be most likely transferred along the L branch.

3.3. Composition of the frontier molecular orbitals

The composition of the frontier molecular orbitals, including HOMO-1, HOMO, LUMO and LUMO + 1, for super-molecules P960 and P960-h were listed in Tables 4 and 5, respectively.

From Tables 4 and 5, it can be seen that, for super-molecules P960, its HOMO-1 and LUMO mainly consist of atomic orbitals of atoms localized at the corresponding composition unit (CU) *BChl* b_L; but its HOMO and LUMO + 1 mainly consist of the atomic orbitals of atoms localized at the CU *BChl* b_M, respectively. In the conditions of the histidine residues coordinating axially to the primary electron donor (P960-h) and the surrounding proteins (SCRF, $\varepsilon = 2.50$) were considered, the composition of HOMO-1, HOMO, LUMO and LUMO + 1 did not change this composition considerably. It is worth pointing out that the influence of the axially coordinated histidine residues on the energy levels of the frontier orbitals of the primary electron donor is significant as mentioned in Sections 3.2 and 3.4.

Let us take a close look at the composition of HOMOs and LUMOs of super-molecules P960 and P960-h. Their HOMOs mainly consist of the atomic orbitals of atoms localized at the pyrrole ring III of the corresponding CUs *BChl* b_M and $BChl\ b_M^h$ molecules, respectively. Histidine residue axial ligands and surrounding proteins (SCRF, $\varepsilon = 2.50$) hardly change this composition. While the LUMOs of P960 and P960-h mainly consist of the atomic orbitals of atoms localized at the pyrrole ring IV of *BChl* b_L and ring I of $BChl\ b_L^h$ molecules, respectively, no matter whether the surrounding proteins are considered or not. These pyrrole rings correspond to photochemical active positions of P960 and P960-h, correspondingly. In a recent paper, Nakatsuji, et al. [26] calculated the electronic structure of primary electron donor P of RC in *Rps. Virid* with the SAC-CI method and concluded that the LUMO of P is slightly localized on the γ-carbon of P_L and the electrons of HOMO in P are located in the upper part of P_M. Fischer, et al. [20] used the INDO/S method and reported that the HOMO and LUMO of P were localized to about 64% and 70% at P_M and P_L, respectively. Our calculated results are in agreement with theirs.

3.4. Mechanism of primary ET

For the mechanism of the primary ET in *Rps. Virid* RC, many researchers have striven to explore the structural chemical background of the fact the ET can only take place along the subunit L, and the current issue is whether the primary ET process is a one-step [15,18,24,25,27,28] or two-step ET process [5,22,29–31]. In this section, the mechanism of primary ET will be studied from the electronic structural point of view.

3.4.1. The direction of primary ET

Let us consider the condition that when super-molecules P960 and P960-h are excited, an electron would be transited from the corresponding HOMOs to the LUMOs. As mentioned above, the LUMOs of super-molecules P960 and P960-h mainly consist of molecular orbitals from *BChl* b_L and $BChl\ b_L^h$, respectively; and the coupling between the special pair P960 and *ABChl* b_L is greater than that between P960 and *ABChl* b_M [4]. Furthermore, the electronic affinities of *BPheo b* and *ABChl b* in the L-branch is also greater than those of the corresponding molecules in M branch mentioned above (Section 3.2). Therefore, the excited electron, localized at the LUMO of P960/P960-h, will be more easily transferred along L-branch, rather than that along M-branch of the bacterial RC. These results are helpful to understand the fact that the primary ET process in RC of *Rps. Virid* only takes place along L-branch.

3.4.2. The role of histidine residue axial ligands of the super-molecule P960-h in the primary ET process

During the process of primary ET in RC of *Rps. Virid*, the transferring electron will be transferred from the primary electron donor P960/P960-h along the LUMOs of pigment molecules sequentially. Table 6 lists the E_{LUMO}s of the super-molecules P960/P960-h, *ABChl b* and *BPheo b* in the RC of *Rps. Virid*.

From Table 6, it can be seen that the E_{LUMO} of P960-h is higher than those of both *ABChl b* and *BPheo b*, but the E_{LUMO} of P960 is much lower than those of *ABChl b* or *BPheo b*. These results indicate that the ET process from P960-h to *ABChl b* or from P960-h to *BPheo b* could take place easily, but the ET process from P960 to *ABChl b* or from P960 to *BPheo b* seems impossible to perform, from the energetic point of view. These results also point out that the coordination of histidine residue axial ligands in super-molecule P960-h plays a key role in the ET process of bacterial photosynthetic RC.

3.4.3. The two-step ET mechanism

Let us define the difference $\Delta E_{LUMO}^{L(M)}$, $\Delta E_{LUMO}^{L(M)} = E_{LUMO}^{P960\text{-}h} - E_{LUMO}^{ABChlb_{L(M)}}$ of E_{LUMO}s between P960-h and *ABChl* b_L, (*ABChl* b_M). From Table 6, it can be seen that ΔE_{LUMO}^{L} (Gas) = ∼2.00 kcal/mol (∼0.087 eV), ΔE_{LUMO}^{L} (SCRF, $\varepsilon = 2.50$) = ∼0.70 kcal/mol (∼0.03 eV), which is good agreement with that (∼1.1 kcal/mol) based on quantum dynamics simulations of experimental data [31] and that (∼0.7 kcal/mol) based on quantum chemical modeling with the B3LYP method in the level of LANL2DZ [34]. The E_{LUMO} of *BPheo* b_L is ca. 1.33 kcal/mol (∼0.058 eV) lower than that of *ABChl* b_L in solution phase (SCRF, $\varepsilon = 2.50$),

Table 4
Compositions of the frontier molecular orbitals of super-molecule P960 (with coefficients of atomic orbital >10%)[a]

Super-molecule		Composition of HOMO-1	Composition of HOMO	Composition of LUMO	Composition of LUMO + 1
P960	GAS	C_4^{2PZ} 0.12967 − N_{33}^{2S} 0.28175 N_{33}^{2PX} 0.17040 − N_{33}^{2PY} 0.37825+ N_{33}^{2PZ} 0.21764 − C_{34}^{2S} 0.24286+ C_{34}^{2PY} 0.19442 + C_{34}^{2PZ} 0.48680+ C_{35}^{2PZ} 0.15578 − C_{36}^{2PZ} 0.12481	N_{80}^{2S} 0.33313 − N_{80}^{2PX} 0.18793+ N_{80}^{2PY} 0.45323 + C_{81}^{2S} 0.28190− C_{81}^{2PY} 0.26637 + C_{81}^{2PZ}0.37907+ C_{82}^{2PZ} 0.10000	$-C_2^{2PZ}$ 0.46012 − N_5^{2S} 0.30987 N_5^{2PX} 0.34905 + N_5^{PY} 0.28995− N_5^{PZ} 0.48909 + C_6^{2PZ} 0.15492 C_8^{2PZ} 0.13010 + C_9^{2S} 0.35169 C_9^{2PY} 0.32297 + C_9^{2PZ} 0.82336+ N_{16}^{2PZ} 0.11238	$-C_{49}^{2PX}$ 0.12969 + C_{49}^{2PZ} 0.47856+ N_{52}^{2PZ} 0.58671 + $-C_{53}^{2PZ}$ 0.13480+ C_{55}^{2PZ} 0.13707 + C_{56}^{2PX} 0.20224− C_{56}^{2PZ} 0.85516 − N_{63}^{2PZ} 0.12632
	SCRF (ε = 2.50)	C_4^{2PZ} 0.12980 − N_{33}^{2S} 0.28171 N_{33}^{2PX} 0.17042 − N_{33}^{2PY} 0.37824+ N_{33}^{2PZ}0.21771 − C_{34}^{2S} 0.24291+ C_{34}^{2PY}0.19445 + C_{34}^{2PZ} 0.48680+ C_{35}^{2PZ}0.15549 − C_{36}^{2PZ}0.12487	C_{51}^{2PZ} 0.16946 − C_{76}^{2PZ} 0.11888 N_{80}^{2S} 0.15192 − N_{80}^{2PY} 0.11344+ N_{80}^{2PZ} 0.35816 + C_{81}^{2S} 0.18208− C_{81}^{2PX} 0.20976 + C_{81}^{2PY} 0.25176+ C_{81}^{2PZ} 0.52076 + C_{81}^{2PZ} 0.26289− C_{83}^{2PZ} 0.13637 − C_{84}^{2PZ} 0.15313	$-C_2^{2PZ}$ 0.45100 − N_5^{2S} 0.34290 N_5^{2PX} 0.36766 + N_5^{PY} 0.32031 N_5^{PZ} 0.47516 + C_6^{2PZ} 0.15288+ C_8^{2PZ} 0.12895 + C_9^{2S} 0.38508+ C_9^{2PY} 0.35719 + C_9^{2PZ} 0.81626+ N_{16}^{2PZ} 0.11101	$-C_{49}^{2PX}$ 0.12949 + C_{49}^{2PZ} 0.47795+ N_{52}^{2PZ} 0.58681 + $-C_{53}^{2PZ}$ 0.13456+ C_{55}^{2PZ} 0.13727 + C_{56}^{2S} 0.20224− C_{56}^{2PZ} 0.85544 − N_{63}^{2PZ} 0.12642

[a] The atoms whose atomic number falls within 0–46 and 47–93 belong to *BChl* b_L and *BChl* b_M, respectively.

Table 5
Compositions of the frontier molecular orbitals of super-molecule P960-h (with coefficients of atomic orbital >10%)[a]

Super-molecule		Composition of HOMO-1	Composition of HOMO	Composition of LUMO	Composition of LUMO + 1
P960	GAS	C_4^{2PZ} 0.12936 − N_{33}^{2S} 0.28157− N_{33}^{2PX} 0.18719 − N_{33}^{2PY} 0.37872+ N_{33}^{2PZ} 0.18707 − C_{34}^{2S} 0.24605+ C_{34}^{2PY} 0.19375 + C_{34}^{2PZ} 0.48623+ C_{35}^{2PZ} 0.15643 − C_{36}^{2PZ} 0.12505	C_{51}^{2PZ} 0.16999 − C_{76}^{2PZ} 0.11790− N_{80}^{2S} 0.12326 + N_{80}^{2PZ} 0.35038+ C_{81}^{2S} 0.17004 − C_{81}^{2PX} 0.25260+ C_{81}^{2PY} 0.23431 + C_{81}^{2PZ} 0.52307− C_{82}^{2X} 0.10542 + C_{82}^{2PZ} 0.26450− C_{83}^{2PZ} 0.13371 − C_{84}^{2PZ} 0.14318	$-C_2^{2PX}$ 0.19148 + C_2^{2PZ} 0.54491− C_3^{2PZ} 0.12677 − N_5^{2PZ} 0.15385+ C_6^{2PZ} 0.10305 − N_{16}^{2PX} 0.17025+ N_{16}^{2PZ} 0.45740 + C_{17}^{2PX} 0.19086− C_{17}^{2PZ} 0.80065 + C_{18}^{2PZ} 0.19086+ C_{19}^{2PZ} 0.14773 − C_{20}^{2PZ} 0.13330	$-C_{49}^{2PZ}$ 0.12191 + C_{50}^{2S} 0.16442− C_{50}^{2PX} 0.25031 − C_{50}^{2PY} 0.17946+ C_{50}^{2PZ} 0.63101 − N_{63}^{2PX} 0.16617+ N_{63}^{2PZ} 0.36668 + C_{65}^{2PZ} 0.10457+ C_{66}^{2PZ} 0.13756 − C_{67}^{2S} 0.17362+ C_{67}^{2PX} 0.28857 − C_{67}^{2PY} 0.10863− C_{67}^{2PZ} 0.78866 − C_{74}^{2PZ} 0.14624
	SCRF (ε = 2.50)	$-C_1^{2S}$ 0.30491 − C_1^{2PX} 0.25236+ C_1^{2PY} 0.24511 + C_1^{2PZ} 0.35706− C_6^{2S}0.27703 − C_6^{2PY}0.14784+ C_6^{2PZ} 0.47323	N_{80}^{2S} 0.33829 − N_{80}^{2PX} 0.18650− N_{80}^{2PY} 0.46288 + C_{81}^{2S} 0.29926+ C_{81}^{2PY} 0.29728 + C_{81}^{2PZ}0.33490	$-C_2^{2PX}$ 0.19177 + C_2^{2PZ} 0.54563− C_3^{2PZ} 0.12690 − N_5^{2PZ} 0.15373+ C_6^{2PZ} 0.10301 − N_{16}^{2PX} 0.16994+ N_{16}^{2PZ} 0.45687 + C_{17}^{2PX} 0.24520− C_{17}^{2PZ} 0.80069 + C_{18}^{2PZ} 0.19057+ C_{19}^{2PZ} 0.14764 − C_{20}^{2PZ} 0.13256	C_{50}^{2PX} 0.16094 − C_{50}^{2PZ} 0.19924+ N_{72}^{2S} 0.61499 − N_{72}^{2PX} 0.42769+ N_{72}^{2PY} 0.26190 − N_{72}^{2PZ} 0.68191− C_{73}^{2S} 0.62584 − C_{73}^{2PX} 0.89481+ C_{73}^{2PY} 0.22733 + C_{73}^{2PZ} 0.26284+ C_{76}^{2PZ} 0.15903

[a] The atoms whose atomic number within 0–46 and 47–93 belong to *BChl* b_L^h and *BChl* b_M^h, respectively. The atoms whose atomic numbers within 94–99 and 100–105 belong to histidine residue axial ligands of *BChl* b_L^h and *BChl* b_M^h molecules, respectively.

Table 6
The LUMO levels for super-molecules P960/P960-h, the accessory bacteriochlorophyll b (*ABChl b*) and pheophytin b (*BPheo b*) in the RC of *Rps. Virid* [a]

	Gas	SCRF ($\varepsilon = 2.50$)
P960	1.97774	1.97311
P960-h	2.48687	2.48088
ABChl b_L	2.40006	2.45013
ABChl b_M	2.48061	2.54156
$ABChl\ b_L^h$	2.83137	2.86946
$ABChl\ b_M^h$	2.91219	2.95273
BPheo b_L	2.37040	2.39217
BPheo b_M	2.43544	2.46483

[a] The subscripts L and M denote the *BChl b* molecules connected with the L and M subunits, respectively. The superscript 'h' represents the histidine residue axial ligands (units eV).

which is consistent with that (∼3 kcal/mol) obtained by Warshel et al [13,32]. On the contrary, $\Delta E_{\mathrm{LUMO}}^{\mathrm{M}}$ (Gas) is ca. ∼0.14 kcal/mol (∼0.0062 eV), and $\Delta E_{\mathrm{LUMO}}^{\mathrm{M}}$ (SCRF, $\varepsilon = 2.50$) is ca. −1.40 kcal/mol (∼0.0607 eV). Those results indicate that the ET process from P960-h to *ABChl* b_L as well as from *ABChl* b_L to *BPheo* b_L could take place, but the ET process from P960-h to *ABChl* b_M seems impossible to take place. This two-step ET process is only

$$P960\text{-}h \xrightarrow{\mathrm{ET}} ABChl\ b_L \xrightarrow{\mathrm{ET}} BPheo\ b_L$$

along the L-branch of *Rps. Virid* RC, which is in agreement with that given in Refs. [5,22,29–31]. Fig. 4 also shows this pathway.

Form the results mentioned above, the primary ET in the RC of *Rps. Virid* can be described as follows:

$$(\mathrm{P960}\text{-}h)(ABChl\ b_L)(BPheo\ b_L) \xrightarrow{h\nu} (\mathrm{P960}\text{-}h)^*(ABChl\ b_L)(BPheo\ b_L)$$

$$(\mathrm{P960}\text{-}h)^*(ABChl\ b_L)(BPheo\ b_L) \xrightarrow{\mathrm{ET}} (\mathrm{P960}\text{-}h)^+(ABChl\ b_L)^-(BPheo\ b_L) \quad (3)$$

$$(\mathrm{P960}\text{-}h)^+(ABChl\ b_L)^-(BPheo\ b_L) \xrightarrow{\mathrm{ET}} (\mathrm{P960}\text{-}h)^+(ABChl\ b_L)(BPheo\ b_L)^-$$

or

$$[(BChl\ b_M^h)(BChl\ b_L^h)](ABChl\ b_L)(BPheo\ b_L) \xrightarrow{h\nu} [(BChl\ b_M^h)^+(BChl\ b_L^h)^-](ABChl\ b_L)(BPheo\ b_L)$$

$$[(BChl\ b_M^h)^+(BChl\ b]_L^h)^-](ABChl\ b_L)(BPheo\ b_L) \xrightarrow{\mathrm{ET}} [(BChl\ b_M^h)^+(BChl\ b_L^h)](ABChl\ b_L)^-(BPheo\ b_L) \quad (4)$$

$$[(BChl\ b_M^h)^+(BChl\ b_L^h)](ABChl\ b_L)^-(BPheo\ b_L) \xrightarrow{\mathrm{ET}} [(BChl\ b_M^h)^+(BChl\ b_L^h)](ABChl\ b_L)(BPheo\ b_L)^-$$

3.4.4. The one-step ET mechanism

In the crystal structure of RC for *Rps. Virid*, the distances between Mg ions in molecules *BChl* b_L, *BChl* b_M, *ABChl* b_L, *ABChl* b_M and N atoms in the corresponding histidine residue axial ligands are 0.22, 0.19, 0.22 and 0.21 nm, respectively. Therefore, the histidine residue axial ligands coordinating with Mg ion of *ABChl b* should be taken into account. Let us define the difference of E_{LUMO}s between P960-h and *ABChl* b_L^h (*ABChl b* $_M^h$) as $\Delta E_{\mathrm{LUMO}}^{\mathrm{L(M)}^h} = E_{\mathrm{LUMO}}^{P960\text{-}h} - E_{\mathrm{LUMO}}^{ABChlb_{\mathrm{L(M)}}^h}$, then we have $\Delta E_{\mathrm{LUMO}}^{L^h}$ (Gas) = −7.94 kcal/mol(−0.345 eV), $\Delta E_{\mathrm{LUMO}}^{L^h}$ (SCRF, $\varepsilon = 2.50$) = −8.96 kcal/mol (−0.389 eV), $\Delta E_{\mathrm{LUMO}}^{M^h}$ (Gas) = −9.81 kcal/mol (−0.425 eV) and $\Delta E_{\mathrm{LUMO}}^{\mathrm{M}^h}$ (SCRF,

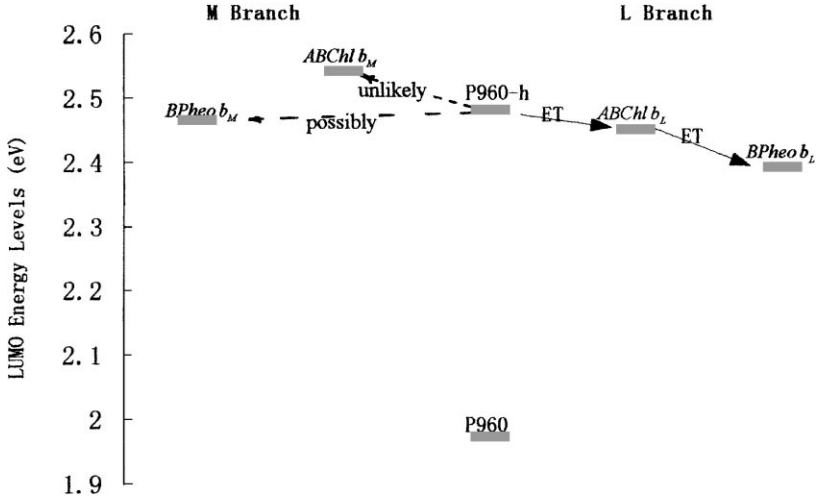

Fig. 4. The energy levels of super-molecules P960/P960-h, the accessory bacteriochlorophyll b (*ABChl b*) and bacteriopheophytin b (*BPheo b*) in solution phase (SCRF, $\varepsilon = 2.50$) as well as the scheme of primary electron transfer pathway.

$\varepsilon = 2.50) = -10.88$ kcal/mol (-0.472 eV), respectively. These results indicate that the ET from P960-h to *ABChl* b_L^h or *ABChl* b_M^h seems impossible to perform. In this case, the primary ET process can only take place from P960-h to *BPheo b*. These results also point out that the coordination of histidine residue axial ligands of *ABChl b* also plays a very important role in the pathway of electron transfer reaction in the RC of *Rps. Virid*.

From Table 6, it can be seen that the differences of LUMO level between P960-h and *BPheo* b_L, are 2.69 kcal/mol ($\sim$0.116 eV) and 2.05 kcal/mol ($\sim$0.0887 eV) in gas and solution phases(SCRF, $\varepsilon = 2.50$), respectively, which are greater than those between P960-h and *BPheo* b_M, 1.18 kcal/mol ($\sim$0.0514 eV) and 0.37 kcal/mol ($\sim$0.0161 eV), respectively. These results indicate that the excited electron from P960-h will be mainly transferred to *BPheo* b_L. Therefore, we could draw a conclusion that the primary ET process in RC of *Rps. Virid* is a one-step process from P960-h to *BPheo* b_L, which is in agreement with that in Refs. [15,18,24,25,27,28]. Fig. 5 also shows the pathway of the one-step primary ET process in RC of *Rps. Virid*. The roles of *ABChl* b_L^h and *ABChl* b_M^h in the primary ET of *Rps. Virid* RC still needs to be studied in the future. The mechanism of the very fast primary ET from the super-molecule P960-h to *BPheo* b_L, as well as the center-to-center distance of $\sim$1.7 nm, in the RC of *Rps. Virid* is still a live subject today.

On the basis of the above analysis, we could conclude that the primary ET in RC of *Rps. Virid* mainly takes place from P960-h to *BPheo* b_L along the L-branch. This one-step primary ET can be described as follows:

$$(\text{P960-}h)(BPheo\ b_L) \xrightarrow{h\nu} (\text{P960-}h)^*(BPheo\ b_L)$$

$$(\text{P960-}h)^*(BPheo\ b_L) \xrightarrow{\text{ET}} (\text{P960-}h)^+(BPheo\ b_L)^- \quad (5)$$

or

$$[(BChl\ b_M^h)(BChl\ b_L^h)](BPheo\ b_L) \xrightarrow{h\nu} [(BChl\ b_M^h)^+(BChl\ b_L^h)^-](BPheo\ b_L)$$

$$[(BChl\ b_M^h)^+(BChl\ b_L^h)^-](BPheo\ b_L) \xrightarrow{ET} [(BChl\ b_M^h)^+(BChl\ b_L^h)](BPheo\ b_L)^- \quad (6)$$

4. Conclusions

From these calculated results mentioned above, the following conclusions can be drawn:

1. For super-molecules P960 and P960-h, the HOMOs mainly consist of the atomic orbitals of atoms localized at the pyrrole ring III of *BChl* b_M and *BChl* b_M^h molecules, respectively. While the LUMOs of P960 and P960-h mainly consist of the atomic orbitals of atoms localized at the pyrrole ring IV of *BChl* b_L and ring I of *BChl* b_L^h molecules, respectively. The surrounding proteins (simulated by SCRF) hardly change the compositions of their HOMO and LUMO. Those factors favor to explain the fact that the primary ET in *Rps. Virid* RC takes place along the L-branch.
2. In the light of the relative positions of E_{LUMO}s of the primary electron donor and other pigment molecules in the RC of *Rps. Virid*, it can be concluded that the primary ET mainly takes place from P960-h to *BPheo* b_L along the L-branch as a one-step process. The coordination of

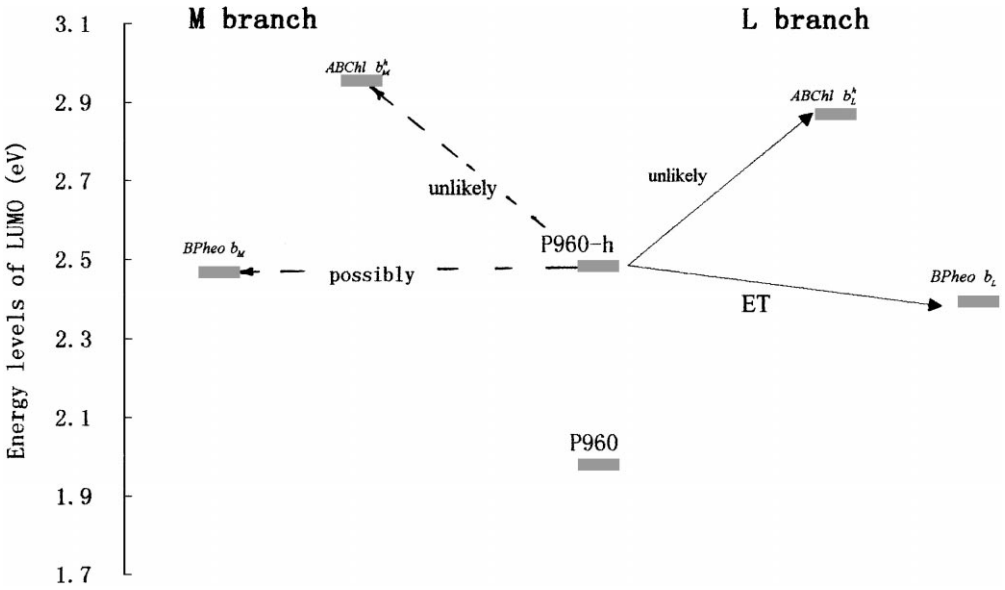

Fig. 5. The energy levels of super-molecules P960/P960-h, the accessory bacteriochlorophyll b with histdine residue axial ligands (*ABChl* b^h) and bacteriopheophytin b (*BPheo b*) in solution phase (SCRF, $\varepsilon = 2.50$) as well as the scheme of primary electron transfer pathway.

histidine residue axial ligands plays a key role in the primary ET of the RC in *Rps. Virid*.

Acknowledgements

The project was supported by the National Natural Science Foundation of China (29733100, 39890390) and the Projects of the State Key Fundamental Research and Development Plan (G1998010100).

References

[1] J. Deisenhefer, O. Epp, K. Mike, R. Huber, H. Michel, Nature 318 (1985) 618.
[2] M.G. Cory, M.C. Zerner, J. Am. Chem. Soc. 118 (1996) 4148.
[3] Toshihiro Sakama, Hiroshi Kashiwagi, Toshikaza Takada, et al., Int. J. Quant. Chem. 61 (1997) 137.
[4] N. Ivashin, B. Kallebring, S. Larsson, O. Hanson, J. Phys. Chem. B 102 (1998) 5017.
[5] L.G. Arnaut, S.J. Formosinho, J. Photochem. Photobiol. A: Chem. 111 (1997) 111.
[6] T. Arlt, S. Schmidt, W. Kaiser, et al., Proc. Nat. Acad. Sci. USA 90 (1993) 11757.
[7] A.R. Holzwarth, M.G. Muller, Biochemistry 35 (1996) 11820.
[8] S. Schmidt, T. Arlt, P. Hamm, et al., Chem. Phys. Lett. 223 (1994) 116.
[9] V. Nagaragan, W.W. Parson, D. Gaul, et al., Proc. Natl. Acad. Sci. USA 87 (1990) 7888.
[10] L.M.P. Beekman, L.H.M. van Stokkum, R. Monshouwer, J. Phys. Chem. 100 (1996) 7256.
[11] M. Huber, Photosyn. Res. 52 (1997) 1–26.
[12] M. Plato, K. Mobius, M.E. Michel-Beyerle, et al., J. Am. Chem. Soc. 110 (1988) 7279.
[13] W.W. Parson, Z. Chu, A. Warshel, Biochim. Biopyhs. Acta 1017 (1990) 251.
[14] M.A. Thompson, M.C. Zerner, J. Fajer, J. Phys. Chem. 94 (1990) 3820.
[15] M.A. Thompson, M.C. Zerner, J. Fajer, J. Phys. Chem. 95 (1991) 5693.
[16] M.A. Thompson, M.C. Zerner, J. Am. Chem. Soc. 110 (1988) 606.
[17] M.A. Thompson, M.C. Zerner, J. Am. Chem. Soc. 112 (1990) 7828.
[18] M.A. Thompson, M.C. Zerner, J. Am. Chem. Soc. 113 (1991) 8210.
[19] P.O.J. Scherer, S.F. Fischer, Chem. Phys. 131 (1989) 115.
[20] P.O.J. Scherer, S.F. Fischer, Chem. Phys. 197 (1995) 333.
[21] P.O.J. Scherer, S.F. Fischer, J. Phys. Chem. 83 (1989) 1633.
[22] N. Makri, E. Sim, D.E. Majarov, M. Topaler, Proc. Nat. Acad. Sci. USA 93 (1996) 3926.
[23] M.A. Steffen, K. Lao, S.G. Boxer, Science 264 (1994) 810.
[24] M. Marchi, J.N. Gehlen, D. Chandler, M. Newton, J. Am. Chem. Soc. 115 (1993) 4178.
[25] M.R. Gunner, A. Nicholls, B. Honig, J. Phys. Chem. 100 (1996) 4277.
[26] J. Hasagawa, H. Nakatsuji, J. Phys. Chem. B 102 (1998) 10420.
[27] G.R. Fleming, J.L. Martin, J. Breton, Nature 335 (1988) 190.
[28] C.K. Chen, T.J. DiMagno, X.Q. Chen, et al., Proc. Nat. Acad. Sci. USA 88 (1991) 11202.
[29] Z. Wang, R.M. Pearlstein, Y. Jia, et al., Chem. Phys. 176 (1993) 421.
[30] Y. Jia, T.J. DiMagno, C.K. Chen, et al., J. Phys. Chem. 97 (1993) 13180.
[31] E. Sim, N. Makri, J. Phys. Chem. B 101 (1997) 5446.
[32] S. Creighton, J.K. Hwang, A. Warshel, et al., Biochemistry 27 (1988) 774.
[33] L. Zhang, R.A. Friesner, J. Phys. Chem. 99 (1995) 16479.
[34] M.R.A. Blomberg, P.E.M. Siegbahn, G.T. Babcock, J. Am. Chem. Soc. 120 (1998) 8812.
[35] J. Fajer, M.S. Davis, D.C. Brune, et al., Brookhaven Symp. Biol 28 (1974) 74.
[36] M.J. Frisch, M. Headgorden, Gaussian 98 (version A.5), Gaussian Inc., Pittsberg, PA, 1999.
[37] M.W. Wong, J.M. Frisch, K.B. Wiberg, J. Am. Chem. Soc. 113 (1991) 4776.